Scientific Journals
of the Maritime University of Szczecin

Zeszyty Naukowe
Akademii Morskiej w Szczecinie

2016, 48 (120), 75–80
ISSN 1733-8670 (Printed)
ISSN 2392-0378 (Online)
DOI: 10.17402/179

Received: 29.04.2016
Accepted: 15.09.2016
Published: 15.12.2016

Wind shear detection based on direct measurements, remote sensing and numerical models

Dariusz Chaładyniak✉, Janusz Jasiński, Sławomir Pietrek, Karolina Krawczyk

Military University of Technology, Faculty of Civil Engineering and Geodesy
Institute of Geodesy, Department of Geographic Information Systems
2 Kaliskiego St., 00-908 Warsaw 49, Poland
e-mail: {dariusz.chaladyniak; janusz.jasinski; slawomir.pietrek; karolina.krawczyk}@wat.edu.pl
✉ corresponding author

Key words: wind shear, vertical air currents, omega equation, sonars, radars, wind profilers, WRF model

Abstract
Wind has huge influence on take-off, landing and cruising of aircraft. Therefore measuring wind direction and speed as well as evaluating its structure are the most important tasks in meteorological support of flights. Wind shear, which is characterized by rapid changes of speed and/or direction, is one of the most hazardous phenomena for aviation. This phenomenon exists mostly in low tropospheric jet streams, areas of active atmospheric fronts, near convective clouds and strong temperature inversions. The paper proves that wind shear is mainly dependent on non-uniform layout of ascending and descending air currents and shows that this phenomenon can be detected by using ground sensors (ultrasonic anemometers), remote sensing methods (sodars, radars, wind profilers) and data from numerical mesoscale models.

Introduction

Scientists of various areas have always been interested in the research of the boundary layer of the atmosphere. Its processes, structure and principal parameters are at the basis of physics of the atmosphere. Theoretical and experimental work has resulted in credible forecasts of atmospheric evolution, making it possible to predict the values of meteorological elements as well as particular types of atmospheric phenomena. This is crucially important when wind structure of its lowest levels is analyzed, especially when wind shear – hazardous for aviation – needs to be detected. Thanks to dynamically developing aviation technology, safer aircraft flights are becoming possible. At the same time, current reports about aviation disasters confirm the great influence of unfavorable weather conditions on take-off and landing, especially as planes have low lift-to-drag ratios.

Vertical air currents

The vertical currents field is one of the most important variables describing the state of the atmosphere. Numerous weather phenomena are caused by ascending or descending air currents. Vertical currents are very important for the development and evolution of pressure systems and frontal zones as well as the formation of cloud systems and precipitation. They are a crucial element of analysis and forecast of the dynamics of pressure systems (Chaładyniak & Jasiński, 2008). The vertical component of the wind field analyzed in the synoptic scale is of the order of a few centimeters per second. Standard meteorological measurements are made with accuracy of 1 m/s. Hence, it is difficult to make direct measurements of vertical currents. This quantity is determined indirectly using wind fields that are measured regularly. Two methods are commonly used to compute vertical currents: kinetic – based on

the continuity equation – and adiabatic – based on the thermodynamic energy equation. Both methods are referenced to an isobaric coordinate system, in which the $\omega(p)$ function is computed according to the following formula:

$$\omega = \frac{Dp}{Dt} = \frac{\partial p}{\partial t} + \mathbf{V} \cdot \nabla p + w\left(\frac{\partial p}{\partial z}\right) \tag{1}$$

written in the (x, y, z) coordinate system.

In large scale atmospheric flows, the horizontal wind is, in first approximation, considered to be geostrophic. We can therefore write that: $\mathbf{V} = \mathbf{V}_g + \mathbf{V}_a$ but $\mathbf{V}_g = (\rho f)^{-1}\mathbf{k}\times\nabla p$, which means that: $\mathbf{V}_g \cdot \nabla p = 0$. We can convert equation (1), using the equation of statics, to obtain:

$$\omega = \frac{\partial p}{\partial t} + \mathbf{V}_a \cdot \nabla p - g\rho w \tag{2}$$

Analyzing the order of the components of the right hand side of equation (2) for large scale atmospheric flows we obtain that the pressure changes during one day are as follows:

$$\partial p/\partial t \sim 10 \text{ hPa}$$

$$\mathbf{V}_a \cdot \nabla p \sim 1 \text{ hPa}$$

$$g\rho w \sim 100 \text{ hPa}$$

Therefore we can use the following approximating relation:

$$\omega = -g\rho w \tag{3}$$

Since geostrophic vorticity, ζ_g, and wind, $\mathbf{V}_g$, can be expressed using only the geopotential, Φ, the following equation:

$$\frac{\partial \zeta_g}{\partial t} = -\mathbf{V}_g \cdot \nabla\left(\zeta_g + f\right) + f_0 \frac{\partial \omega}{\partial p} \tag{4}$$

can be used to analyze vertical currents fields, ω, when the Φ and $\partial\Phi/\partial t$ fields are available. Geopotential tendency, $\chi = \partial\Phi/\partial t$, is a basic forecast field used operationally in weather services. Despite the fact that upper air levels analyses are available only twice a day, the tendency approximation based on observations of geopotential at 12-hour intervals provides more accurate forecasts than other methods in use. This paper presents an alternative method based on vorticity and thermodynamic equations.

Omega equation

The omega equation was first presented by J.G. Charney in 1947. It enables to determine vertical currents fields, ω, exclusively on the basis of the spatial distribution of geopotential. To derive the omega equation we can use the mathematical definition of the baroclinic model (Charney, 1947):

$$\frac{\partial \chi}{\partial p} = -\mathbf{V}_g \cdot \nabla\left(\frac{\partial \Phi}{\partial p}\right) - \sigma\omega \tag{5}$$

where σ is the parameter of the static stability of the atmosphere in the quasi-geostrophic approximation:

$$\nabla^2 \chi = -f_0 \mathbf{V}_g \cdot \nabla\left(\frac{1}{f_0}\nabla^2\Phi + f\right) + f_0^2 \frac{\partial \omega}{\partial p} \tag{6}$$

The procedure proposed in the paper consists in eliminating the geopotential tendency χ from the above system of functions. To achieve this, we apply the ∇^2 operator to equation (5):

$$\nabla^2\left(\frac{\partial \chi}{\partial p}\right) = -\nabla^2\left[\mathbf{V}_g \cdot \nabla\left(\frac{\partial \Phi}{\partial p}\right)\right] - \sigma\nabla^2\omega \tag{7}$$

and we differentiate equation (6) against pressure, p:

$$\frac{\partial}{\partial p}\left(\nabla^2\chi\right) = -f_0 \frac{\partial}{\partial p}\left[\mathbf{V}_g \cdot \nabla\left(\frac{1}{f_0}\nabla^2\Phi + f\right)\right] + f_0^2 \frac{\partial^2 \omega}{\partial p^2} \tag{8}$$

Since $$\nabla^2\left(\frac{\partial \chi}{\partial p}\right) = \frac{\partial}{\partial p}\left(\nabla^2\chi\right)$$

the differential operators on the right side of equations (7) and (8) are equal, that the term $\nabla^2(\partial\chi/\partial p)$ can be eliminated, resulting in:

$$\underbrace{\left(\nabla^2 + \frac{f_0^2}{\sigma}\frac{\partial^2}{\partial p^2}\right)\omega}_{\text{A}} = \underbrace{\frac{f_0}{\sigma}\frac{\partial}{\partial p}\left[\mathbf{V}_g \cdot \nabla\left(\frac{1}{f_0}\nabla^2\Phi + f\right)\right]}_{\text{B}} + \underbrace{\frac{1}{\sigma}\nabla^2\left[\mathbf{V}_g \cdot \nabla\left(-\frac{\partial \Phi}{\partial p}\right)\right]}_{\text{C}} \tag{9}$$

Equation (9) is the so-called classical omega equation and it only contains derivatives with respect to the spatial variables. This equation defines a method of determining the ω function that, unlike the continuity equation, is independent of the ageostrophic component of the wind field:

$$\nabla \cdot \mathbf{V}_a + \frac{\partial \omega}{\partial p} = 0 \tag{10}$$

By integrating equation (10) with respect to pressure we obtain:

$$\omega(p) - \omega(p_s) = \int_{p_s}^{p}\left(\frac{\partial u_a}{\partial x} + \frac{\partial v_a}{\partial y}\right)\mathrm{d}\,p \tag{11}$$

where p_s is the reference pressure (e.g. 1000 hPa or surface pressure) and p is the pressure at a selected level.

Hence, direct measurements of wind are not necessary. Equation (9) does not require information on the distribution of vorticity tendency. This means that in order to determine the ω field, it is sufficient to know the distribution of geopotential for a single observation time. On the other hand, the analyzed equation includes second order derivatives with respect to the vertical coordinate. The precise assessment of the specific expressions through measurement data characterized by noise may be a very difficult task. The left side of equation (9) is not a classical Laplace operator and the σ coefficient that appears at the vertical coordinate is dependent on static stability of the atmosphere. Analysis of components in the omega equation (9) shows that the differential operator defined as A (with the assumption that σ = const.) corresponds to operator A in the geopotential tendency equation (Hoskins, Draghici & Davis, 1978):

$$\underbrace{\left[\nabla^2+\frac{\partial}{\partial p}\left(\frac{f_0^2}{\sigma}\frac{\partial}{\partial p}\right)\right]}_{\text{A}}\chi=\underbrace{-f_0\mathbf{V}_g\cdot\nabla\left(\frac{1}{f_0}\nabla^2\Phi+f\right)}_{\text{B}}+\underbrace{-\frac{\partial}{\partial p}\left[-\frac{f_0^2}{\sigma}\mathbf{V}_g\cdot\nabla\left(-\frac{\partial\Phi}{\partial p}\right)\right]}_{\text{C}} \tag{12}$$

$$\text{i.e.: } \nabla^2+\frac{\partial}{\partial p}\left(\frac{f_0^2}{\sigma}\frac{\partial}{\partial p}\right)=\nabla^2+\frac{f_0^2}{\sigma}\frac{\partial^2}{\partial p^2}.$$

Since the forces defined on the right hand side of equation (9) have their maxima in the middle of the troposphere and the ω function equals zero at the lower and upper boundaries of the atmosphere, it is possible to assume that ω has sinusoidal courses both in the horizontal plane and along the vertical axis:

$$\omega=W_0\sin(\pi p/p_0)\sin kx\sin ly \tag{13}$$

Introducing solution (13) to equation (9) gives:

$$\left(\nabla^2+\frac{f_0^2}{\sigma}\frac{\partial^2}{\partial p^2}\right)\omega\approx-\left[k^2+l^2+\frac{1}{\sigma}\left(\frac{f_0\pi}{p_0}\right)^2\right]\omega \tag{14}$$

Expression A is thus proportional to $-\omega$. Having in mind that ω is proportional to $-\omega$ (see equation (5)), we conclude that $\omega < 0$ results in ascending air currents and consequently A is proportional to vertical velocity. This means that positive values of the sum of B and C result in ascending air currents, while negative values result in descending currents. Expression B in equation (12) is called total vorticity advection. Expression B in equation (9) is proportional to the value of the increase of the total vorticity advection with altitude and it is sometimes called differential vorticity. Figure 1 illustrates that:

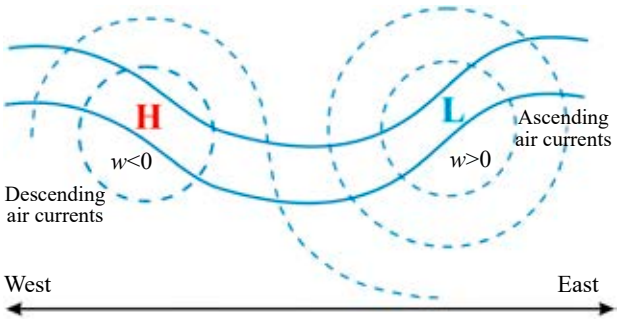

Figure 1. Geopotential of the 500 hPa (solid line) and the 1000 hPa (dashed line) level surfaces presenting areas of strong vertical movements caused by total vorticity advection. H – high pressure area, L – low pressure area (Holton, 1992)

$$w\propto\left\{\frac{\partial}{\partial z}\left[-\mathbf{V}_g\cdot\nabla(\zeta_g+f)\right]\right.$$
$$<0 \text{ over a high pressure area H}$$
$$>0 \text{ over a high pressure area L} \tag{15}$$

The total vorticity advection therefore corresponds to ascending air currents over ground low pressure areas and descending air currents over ground high pressure areas. Expression C in equation (12) is the horizontal Laplace function of the specific volume advection. The vertical velocity value due to this component can be determined by means of the following formula:

$$w\propto\nabla^2\left[\mathbf{V}_g\cdot\nabla\left(-\frac{\partial\Phi}{\partial p}\right)\right]\propto-\mathbf{V}_g\cdot\nabla\left(-\frac{\partial\Phi}{\partial p}\right) \tag{16}$$

In case of warm air advection, expression C is positive. Hence, for very weak or inexistent total vorticity advection, the vertical velocity, ω, is also positive. For cold air advection, expression C is negative. Hence, for very weak or inexistent total vorticity advection, the vertical velocity, ω, is also negative.

Figure 2 illustrates ascending currents occur on the eastern side of a ground low pressure system in the area of the warm front while descending currents occur behind the cold front on the western side of the ground low pressure system. Further analysis indicates that the vertical currents and temperature advection sustain the geostrophic character of the

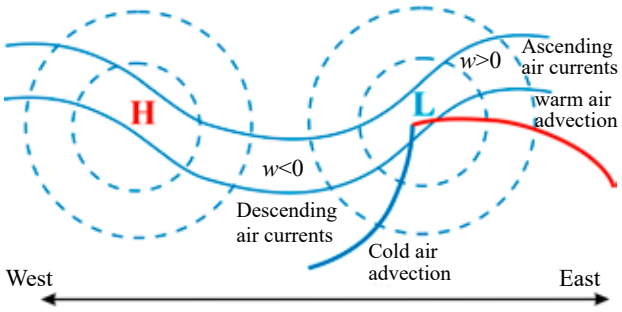

Figure 2. Geopotential of the 500 hPa (solid line) and the 1000 hPa (dashed line) level surfaces presenting areas of strong vertical movements caused by temperature advection. H – high pressure area, L – low pressure area (Holton, 1992)

upper vorticity field. Warm air advection increases the thickness of the 500/1000 hPa layer in the area of an upper ridge at the 500 hPa surface. The geopotential increases and anti-cyclonic vorticity in the region of the ridge guarantee the preservation of geostrophic balance. Since vorticity advection cannot increase the anti-cyclonic vorticity in the upper ridge, the horizontal divergence has to balance the negative tendency of vorticity. According to mass conservation, divergence of the upper vorticity field is compensated by ascending air currents. Descending currents occur in the area of the trough at the 500 hPa surface (cold air advection region).

Wind shear

Wind shear poses the greatest threat to aircraft during take-off and landing. Wind shear may result in changing flight path or throwing off aerodynamic balance. According to ICAO, among all accidents occurring during landing, wind shear is responsible for over 20% of cases in which the aircrafts drive off the runway and 10% of short landings. This information itself shows how important wind shear detection is for direct meteorological support. Airport systems are required to provide credible information about the threat of wind shear occurrence so that decisions about continuing or breaking the take-off or landing procedures can be made. The detection of wind shear using only ground sensors is extremely difficult because of its limited space and short time of occurrence, justifying the efforts of meteorologists to find more credible methods for wind shear detection. Several observations have allowed to conclude that a strong stream of descending air is formed near convective clouds, and its speed can be as high as 75–110 km/h or even 135 km/h. When the stream reaches the ground it flows horizontally in all directions, creating strong whirls of air within 2–5 km radius of the center of the descending stream and up to 600 meters above the ground. The maximum speed of the flowing air is estimated at 100 km/h (Djurić, 1994). The mechanism of wind shear creation and flying in such conditions are presented in the Figures 3 and 4.

We now move on to analyze the case of wind speed increase with height. During landing, the plane travelling into wind enters into the lower layers with weaker head wind, therefore its lift decreases gradually. As a result, the plane's actual line of flight runs below the assumed approach path, the aircraft gets mushing and despite increased drag the landing may

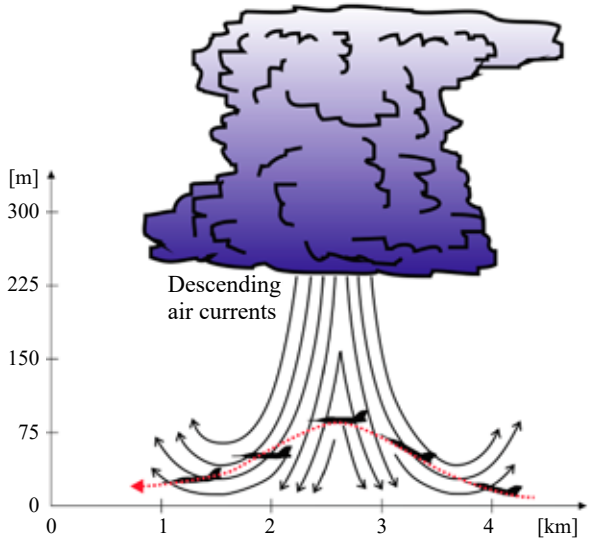

Figure 3. Influence of strong descending air currents on a flying aircraft

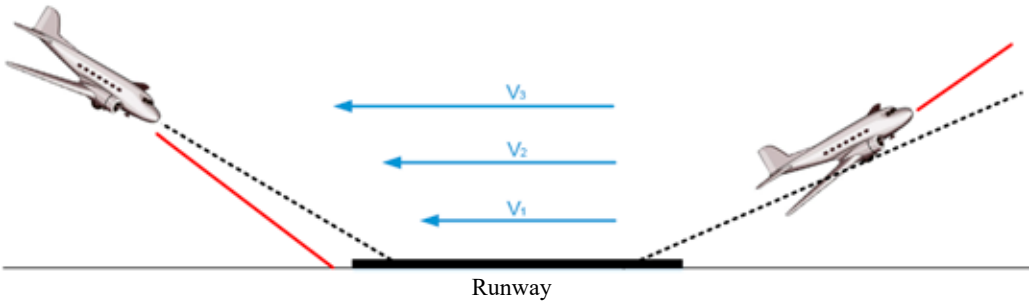

Figure 4. Influence of wind shear on take-off and landing. Expected (dashed line) and actual (solid line) flight path

be short. During take-off, the ascending aircraft gets into layers with stronger head wind and it is affected by stronger lift than in lower layers. Therefore its actual take-off path angle is higher than expected. This may result in exceeding the stalling angle and mushing of the aircraft.

During take-off and landing the speed of an aircraft fluctuates between 200 and 280 km/h. When the aircraft is flying through descending air currents it is subjected to winds of different speeds and directions. Sudden short-term changes in airspeed of the plane result in rapid increase and decrease of lift, which are especially dangerous at low altitudes and at low speed.

Wind shear detection

A few methods of detecting wind shear exist. The following are some examples of equipment used to acquire data for assessing the wind conditions favorable for the phenomenon (Figures 5–8).

Figure 5. Ultrasonic anemometer

Figure 6. Sodar (Schwechat airport)

Figure 7. Radar wind profiler (White Sands, USAF)

Figure 8. Radar (Brzuchania)

Vertical air current field layouts acquired from the WRF (Weather Research and Forecasting) numerical mesoscale model are presented in the Figures 9–11.

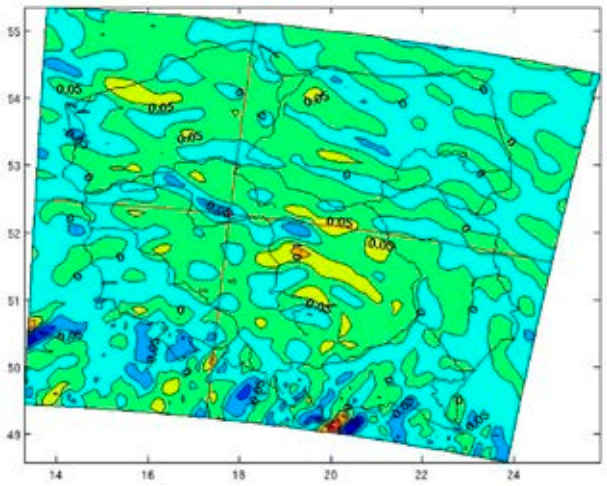

Figure 9. Field of the vertical component of wind speed at the 10th computational surface of the WRF model

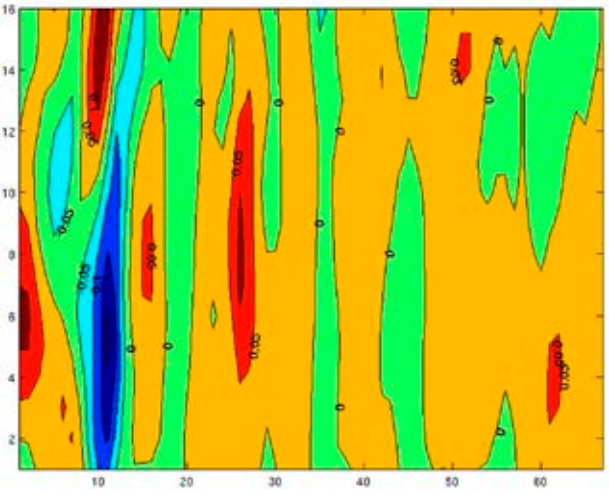

Figure 10. Vertical component of wind speed profile along a meridional line

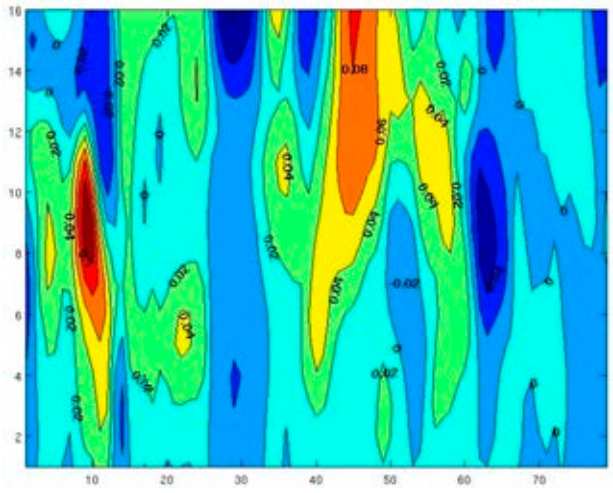

Figure 11. Vertical component of wind speed profile along a latitudinal line

Conclusions

The information provided here shows how important wind shear detection is for direct meteorological support. Airport meteorological measurement systems are required to provide credible information on the probability of occurrence of wind shear so that decisions on continuing or aborting take-off or landing can be made. The wind shear phenomenon is almost impossible to detect by using only ground sensors (ultrasonic anemometers) due to its limited range and brief occurrence. Therefore, one can understand the meteorologists' efforts to find credible wind shear detection methods. In cases where direct measuring is technically problematic or impossible because of the area size, remote sensing methods (sodars, radars, wind profilers) become especially important. Effective and credible detection of wind shear is also possible based on detailed analysis of vertical air current fields available from numerical weather prediction models.

Acknowledgments

The research was conducted and the paper was prepared by the personnel of the Department of Geographic Information Systems within Research project No. 23-933.

References

1. Chaładyniak, D. & Jasiński, J. (2008) Vertical air currents assessment for meteorological support of airborne missions of data acquisition for GIS. *Polish Journal of Environmental Studies*, *Hard Olsztyn* 17, 1C. pp. 19–22.
2. Charney, J.G. (1947) The dynamics of long waves in baroclinic westerly current. *J. Meteor*. 4, 5. pp. 135–162.
3. Djurić, D. (1994) *Weather analysis*. New Jersey: Prentice Hall, Englewood Cliffs.
4. Holton, J.R. (1992) *An introduction to dynamic meteorology*. Third edition. San Diego: Academic Press.
5. Hoskins, B.J., Draghici, I. & Davies, H.C. (1978) A new look at the ω-equation. *Quart. J. Roy. Meteorol. Soc*. 104. pp. 31–38.